Journal of Materials Processing Technology 148 (2004) 226–234

Journal of Materials Processing Technology

www.elsevier.com/locate/jmatprotec

Computerized tooth profile generation and analysis of characteristics of elliptical gears with circular-arc teeth

Chien-Fa Chen, Chung-Biau Tsay*

Department of Mechanical Engineering, National Chiao Tung University, Hsinchu 30010, Taiwan, ROC

Received 2 December 2002; accepted 29 July 2003

Abstract

This study describes rack cutters with circular-arc profile teeth to generate elliptical gears which rotate about one of their foci. A mathematical model for elliptical gears with circular-arc teeth is developed according to gear theory. The influence of the design parameters, such as the number of teeth, gear module, pressure angle at the pitch point and the major-axis, are investigated. The effects of the circular-arc radius of the rack cutter on both the undercutting of teeth and on pointed teeth of the generated circular-arc elliptical gear are also studied. Three numerical examples are presented to elucidate the generation of gear tooth profiles using the proposed mathematical model, and to investigate the phenomena of tooth undercutting and pointed teeth.
© 2003 Published by Elsevier B.V.

Keywords: Elliptical gear; Mathematical model; Circular-arc teeth; Tooth undercutting; Pointed teeth

1. Introduction

Irregular rotational motion of a gear is characterized by a recurrent increase and decrease in the output-shaft rotational speed during each revolution. Several mechanisms, such as drag-links, cycloidal cranks and cyclic three-gear drives, are utilized to produce irregular rotational motion. However, noncircular gears are preferred. The elliptical gear is a noncircular gear whose pitch curve is an ellipse. The elliptical gear, while being kinematically equivalent to the crossed-link, does not have such a connecting link, and thus yields a higher rotational speed. The elliptical gear is well known for its favorable characteristics such as compact size, accurate transmission and easy dynamic balance. Hence, the elliptical gear is the most commonly used noncircular gear in automatic machinery, flying shears, pumps, flow meters and other instruments.

Several studies of elliptical gears [1–4] have focused on kinematic analysis and computer-aided design of elliptical pitch curves. Freudenstein and Chen [5] developed variable-ratio chain drives, and applied them to bicycles and variable motion transmission involving band drives, tape drives and time belts with a minimum slack. Kuczewski [6] transformed an elliptical gear into an equivalent circular gear to approximate the profile of an ellipical gear. Emura and Arakawa [7] employed elliptical gears to analyze a steering mechanism able to turn a carrier with a small radius. Litvin [8] developed extending tooth evolute curves to form a tooth profile, and also derived the tooth evolute of an ellipse. Chang et al. [9] employed gear theory and the geometry of a straight-sided rack cutter to derive a mathematical model for elliptical gears, in which the number of teeth had to be odd, and also examined the undercutting conditions of the developed elliptical gears.

Nieman and Hayer [10] investigated Flender-type worms with concave–convex surfaces. Circular-arc helical gears have been proposed by Wildhaber [11] and Novikov [12]. Litvin and Tsay [13] investigated the kinematic errors of a single circular-arc helical gear drive under various assembly conditions, and improved the bearing contact by correcting the tool settings. Litvin [8] also studied the generation, geometry, meshing and contact of double circular-arc helical gears. Ariga and Nagata [14] used a cutter with combined circular-arc and involute tooth profiles to generate a new type of Wildhaber–Novikov (W–N) gear. This W–N gear has a long fatigue life and is insensitive to center distance variations. Tsay et al. [15] applied the finite element method to analyze the stress of W–N gears.

No mathematical model of an elliptical gear with a circular-arc profile has yet been described in the literature. This study simulates the manufacture of elliptical gears

* Corresponding author. Tel./fax: +886-3-572-8450.
E-mail address: cbtsay@mail.nctu.edu.tw (C.-B. Tsay).

0924-0136/$ – see front matter © 2003 Published by Elsevier B.V.
doi:10.1016/j.jmatprotec.2003.07.011

cut by convex and concave circular-arc rack cutters on a hobbing machine. The cutting mechanism is considered to be such that the rotation shaft of the ellipse coincides with one of the elliptical foci, and that the rack cutter performs a pure rolling on the pitch curve of the ellipse and translates along the tangent direction to the pitch curve. Based on gear theory and the proposed generation mechanism, a mathematical model of the circular-arc elliptical gear is developed. The proposed method here can be applied to generate the elliptical gear tooth profile regardless of whether the number of gear teeth is odd or even. Furthermore, several special gear characteristics, such as undercutting and pointed teeth, are considered due to the complex tooth profile of the circular-arc elliptical gear. Mathematically, tooth undercutting occurs when a singular point appears on the generated elliptical gear tooth surface. The design parameters of the rack cutter must be limited to avoid tooth undercutting. Pointed teeth may also appear when the right- and left-side of the circular-arc tooth profiles intersect each other on or under the addendum circle. Usually, pointed teeth are generated on the major-axis of an elliptical gear else no pointed teeth are generated over any of the elliptical gear profile. This study offers two indexes to predict the occurrence of tooth undercutting and pointed teeth of the elliptical gear under various design parameters. A computer program is developed to provide proper design parameters for the designed circular-arc elliptical gear to avoid tooth undercutting and pointed teeth on the generated tooth profile.

2. Pitch curve of elliptical gear

Fig. 1 shows the geometric relationship of an elliptical gear, which is rotated about one of its foci. Based on these geometric relations, the pitch curve of ellipse $r_j(\phi_j)$ can be represented in the polar coordinate system by the following equation [16]:

$$r_j(\phi_j) = \frac{b_j^2}{a_j(1+\varepsilon_j\cos\phi_j)}, \tag{1}$$

where $j = 1, 2$ and $\phi_2 = \phi_1 + \pi$.

In Eq. (1), parameter $\varepsilon_j = (a_j^2 - b_j^2)^{1/2}/a_j$ is the eccentricity of the ellipse, a_j the length of the major semi-axis, and b_j the length of the minor semi-axis. The position vector of the pitch curve of the ellipse, $r_j(\phi_j)$, can also be represented in the Cartesian coordinate system as follows:

$$x_j = \frac{b_j^2\cos\phi_j}{a_j(1+\varepsilon_j\cos\phi_j)}, \tag{2}$$

and

$$y_j = \frac{b_j^2\sin\phi_j}{a_j(1+\varepsilon_j\cos\phi_j)}. \tag{3}$$

The unit tangent vector of the pitch curve can be determined by differentiating Eqs. (2) and (3) with respect to parameter ϕ_j and then normalizing the results. Therefore,

$$\boldsymbol{\tau}_j = \frac{-\sin\phi_j}{(1+2\varepsilon_j\cos\phi_j+\varepsilon_j^2)^{1/2}}\boldsymbol{i}_j + \frac{\varepsilon_j+\cos\phi_j}{(1+2\varepsilon_j\cos\phi_j+\varepsilon_j^2)^{1/2}}\boldsymbol{j}_j. \tag{4}$$

According to Fig. 1, the unit tangent vector, $\boldsymbol{\tau}_j$, of the pitch curve can also be represented in terms of the tangent angle, γ_j, by the following equation:

$$\boldsymbol{\tau}_j = \cos\gamma_j\boldsymbol{i}_j + \sin\gamma_j\boldsymbol{j}_j. \tag{5}$$

Based on Eqs. (4) and (5), the relationship between γ_j and ϕ_j can be expressed as

$$\cos\gamma_j = \frac{-\sin\phi_j}{(1+2\varepsilon_j\cos\phi_j+\varepsilon_j^2)^{1/2}}, \tag{6}$$

and

$$\sin\gamma_j = \frac{\varepsilon_j+\cos\phi_j}{(1+2\varepsilon_j\cos\phi_j+\varepsilon_j^2)^{1/2}}. \tag{7}$$

The unit normal vectors can be obtained by

$$\boldsymbol{n}_j = \boldsymbol{\tau}_j \times \boldsymbol{k}_j = \sin\gamma_j\boldsymbol{i}_j - \cos\gamma_j\boldsymbol{j}_j.$$

The arc length from the pitch point, I, to the starting point, M, along the pitch curve of the ellipse can be calculated as follows:

$$S_{\mathrm{MI}} = \int_0^{\phi_j}\sqrt{r_j^2+\left(\frac{\mathrm{d}r_j}{\mathrm{d}\phi_j}\right)}\,\mathrm{d}\phi_j = \int_0^{\phi_j}\frac{a_j(1-\varepsilon_j^2)\sqrt{1+2\varepsilon_j\cos\phi_j+\varepsilon_j^2}}{(1+\varepsilon_j\cos\phi_j)^2}\,\mathrm{d}\phi_j. \tag{8}$$

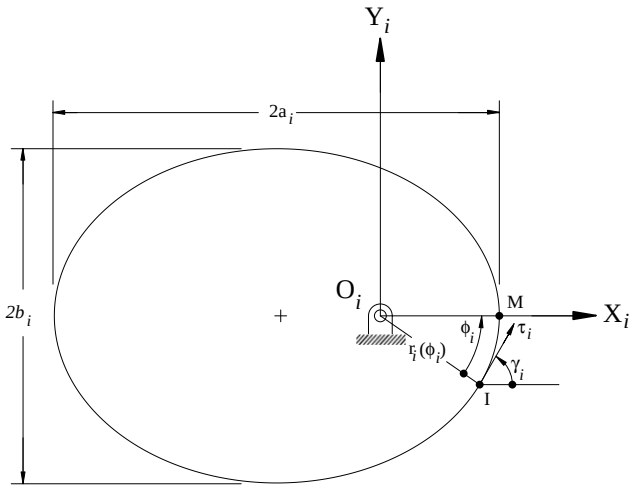

Fig. 1. Tangent line of the elliptical pitch curve.

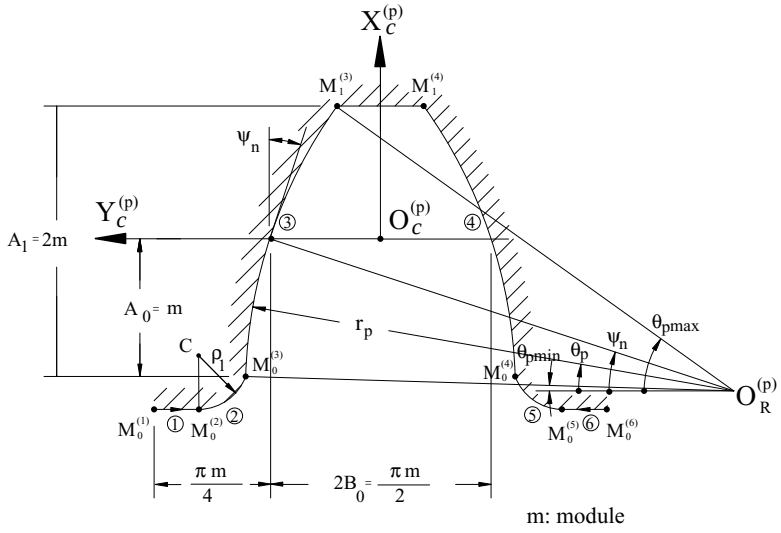

Fig. 2. Normal section of rack cutter Σ_p for generating the driving elliptical gear.

3. Generating surfaces

In this work, rack cutters with convex and concave shapes are designed to generate driving and the driven gears, respectively. Fig. 2 displays a normal section of the circular-arc rack cutter, Σ_p, for generating of the driving elliptical gear, where regions 3 and 4 cut the left- and right-side working regions of the gear; regions 2 and 5 generate the left- and right-side fillets, and regions 1 and 6 generate the left- and right-side top lands, respectively. In Fig. 2, parameter r_p is the radius of the circular-arc rack cutter, parameter θ_p is the angle measured from the horizontal line to an arbitrary location on the working region, and U_p is the width of the rack cutter profile. Based on the geometry of the rack cutter shown in Fig. 2, the working region of the rack cutter can be expressed in the $S_c^{(p)}(X_c^{(p)}, Y_c^{(p)}, Z_c^{(p)})$ coordinate system by the following equation:

$$\boldsymbol{R}_c^{(p)} = \begin{bmatrix} r_p(\sin\theta_p - \sin\psi_n) \\ \pm[r_p(\cos\theta_p - \cos\psi_n) + B_0] \\ U_p \end{bmatrix}. \tag{9}$$

The upper sign of Eq. (9) indicates the left-side circular-arc rack cutter surface, while the lower sign represents the right-side circular-arc rack cutter surface. Parameter B_0 represents the tooth thickness of the elliptical gear, and ψ_n represents the pressure angle measured at the pitch point. The surface unit normal vector to the working region of the rack cutter surface can be obtained by equation

$$\boldsymbol{n}_c^{(i)} = \frac{\boldsymbol{N}_c^{(i)}}{|\boldsymbol{N}_c^{(i)}|}, \tag{10}$$

where $\boldsymbol{N}_c^{(i)} = (\partial \boldsymbol{R}_c^{(i)}/\partial\theta_i) \times \boldsymbol{k}_c^{(i)}$, and $i = p, g$.

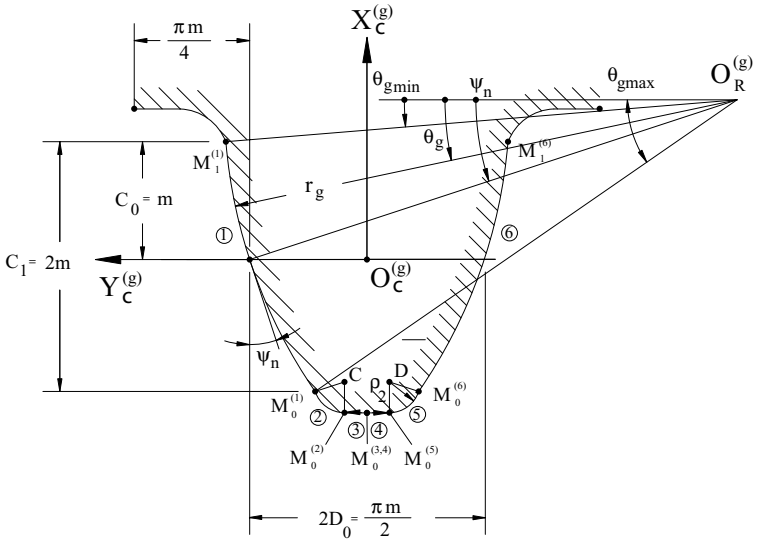

Fig. 3. Normal section of rack cutter Σ_g for generating the driving elliptical gear.

Eqs. (9) and (10) yield the surface unit normal vector of the working region of the rack cutter, Σ_p, as follows:

$$\boldsymbol{n}_c^{(p)} = \begin{bmatrix} \sin\theta_p \\ \pm\cos\theta_p \\ 0 \end{bmatrix}. \tag{11}$$

The other circular-arc rack cutter Σ_g, whose cross-section is illustrated in Fig. 3, is designed to generate the driven circular-arc elliptical gear. Similarly, the working regions of the circular-arc rack cutter, Σ_g, can be represented in the $S_c^{(g)}(X_c^{(g)}, Y_c^{(g)}, Z_c^{(g)})$ coordinate system as follows:

$$\boldsymbol{R}_c^{(g)} = \begin{bmatrix} r_g(\sin\psi_n - \sin\theta_g) \\ \pm[r_g(\cos\theta_g - \cos\psi_n) + D_0] \\ U_g \end{bmatrix}. \tag{12}$$

Substituting Eq. (12) into Eq. (10) yields the unit normal vector of the rack cutter Σ_g:

$$\boldsymbol{n}_c^{(g)} = \begin{bmatrix} -\sin\theta_g \\ \pm\cos\theta_g \\ 0 \end{bmatrix}. \tag{13}$$

4. Generated tooth surfaces

Fig. 4 depicts the generation mechanism for an elliptical gear. The coordinate system $S_c^{(p)}(X_c^{(p)}, Y_c^{(p)}, Z_c^{(p)})$ is attached to the rack cutter, Σ_p, and the coordinate system $S_1(X_1, Y_1, Z_1)$ is attached to the generated elliptical gear, whose rotation centre coincides with one of its foci. Parameter γ_1 is the angle formed by axes $Y_c^{(p)}$ and X_1. The rotation angle of the elliptical gear is $\pi/2 - \gamma_1$, and angle ϕ_1 is a function of γ_1. Parameter S denotes the translational distance, measured along the pitch line of the rack cutter, from the instantaneous pitch point, I, to the origin, $O_c^{(p)}$, of the coordinate system $S_c^{(p)}$. When the circular-arc rack cutter cuts the elliptical gear, the motion of the rack cutter and the generated gear purely roll without sliding on the pitch ellipse, and the rack cutter simultaneously translates along the $X_c^{(p)}$-axis and $Y_c^{(p)}$-axis, while the gear blank rotates about one of the foci of the pitch ellipse. Based on gear theory, the generated elliptical gear surface can be obtained by simultaneously considering the equation of meshing and the locus of the imaginary rack cutter represented in coordinate system S_1. Therefore, the mathematical model of the generated elliptical gear tooth surface can be obtained by applying the following equations [8]:

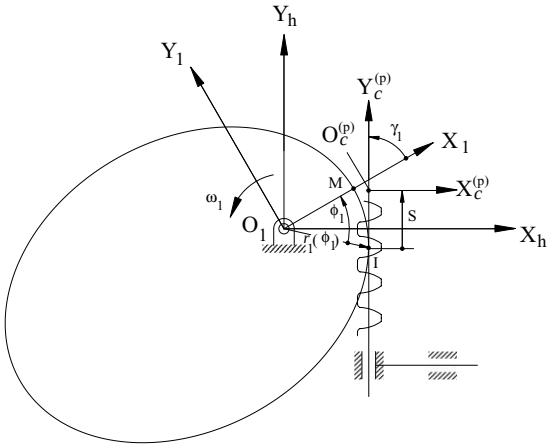

Fig. 4. Kinematic relationship between rack cutter and generated gear.

$$\boldsymbol{R}_1 = [M_{1c}]\boldsymbol{R}_c^{(p)}, \tag{14}$$

and

$$\frac{X_{c,I}^{(p)} - x_c^{(p)}}{n_{xc}^{(p)}} = \frac{Y_{c,I}^{(p)} - y_c^{(p)}}{n_{yc}^{(p)}}, \tag{15}$$

where

$$[M_{1c}] = \begin{bmatrix} \sin\gamma_1 & \cos\gamma_1 & 0 & r_1\cos\phi_1 + S\cos\gamma_1 \\ -\cos\gamma_1 & \sin\gamma_1 & 0 & -r_1\sin\phi_1 + S\sin\gamma_1 \\ 0 & 0 & 1 & 0 \\ 0 & 0 & 0 & 1 \end{bmatrix},$$

and $X_{c,I}^{(p)} = 0$ and $Y_{c,I}^{(p)} = -S$ are coordinates of the pitch point I, $x_c^{(p)}$ and $y_c^{(p)}$ denote the coordinates of the instantaneous point of contact on the rack cutter surface, Σ_p, and $n_{xc}^{(p)}$ and $n_{yc}^{(p)}$ are the unit normal vectors of the contact point, represented in coordinate system $S_c^{(p)}$. Eq. (15) is the so-called equation of meshing for the rack cutter and the generated gear.

Substituting Eqs. (9) and (11) into Eqs. (14) and (15) yields the driving elliptical gear tooth surface as follows:

$$\boldsymbol{R}_1 = \begin{bmatrix} B_1\sin\gamma_1 + C_1\cos\gamma_1 + r_1\cos\phi_1 + S\cos\gamma_1 \\ -B_1\cos\gamma_1 + C_1\sin\gamma_1 - r_1\sin\phi_1 + S\sin\gamma_1 \\ U_p \end{bmatrix}, \tag{16}$$

and

$$\pm S\sin\theta_p = r_p\sin(\theta_p - \psi_n) - B_0\sin\theta_p, \tag{17}$$

where

$$B_1 = r_p(\sin\theta_p - \sin\psi_n),$$
$$C_1 = \pm[r_p(\cos\theta_p - \cos\psi_n) + B_0],$$

and r_1 and r_p are the radii of the elliptical pitch curve and the circular-arc rack cutter Σ_p, respectively, and θ_p is a design parameter of the rack cutter, Σ_p, used to define the working region of the driving gear and limited by $\theta_{p\min} \le \theta_p \le \theta_{p\max}$, as shown in Fig. 2. The limited values are represented by the following equations:

$$\theta_{p\min} = \sin^{-1}\left(\frac{r_p\sin\psi_n - A_0}{r_p}\right), \tag{18}$$

and

$$\theta_{\mathrm{p}\max} = \sin^{-1}\left(\frac{r_{\mathrm{p}}\sin\psi_{\mathrm{n}} - A_0 + A_1}{r_{\mathrm{p}}}\right). \tag{19}$$

In Eq. (17), the upper sign denotes the left-side circular-arc elliptical gear surface while the lower sign represents the right-side gear surface.

The mathematical model of the driven circular-arc elliptical gear can be similarly derived and represented in coordinate system $S_2(X_2, Y_2, Z_2)$ as follows:

$$\boldsymbol{R}_2 = \begin{bmatrix} B_2\sin\gamma_2 + C_2\cos\gamma_2 + r_2\cos\phi_2 + S\cos\gamma_2 \\ -B_2\cos\gamma_2 + C_2\sin\gamma_2 - r_2\sin\phi_2 + S\sin\gamma_2 \\ U_{\mathrm{g}} \end{bmatrix}, \tag{20}$$

and

$$\pm S\sin\theta_{\mathrm{g}} = r_{\mathrm{g}}\sin(\theta_{\mathrm{g}} - \psi_{\mathrm{n}}) - D_0\sin\theta_{\mathrm{g}}, \tag{21}$$

where

$$B_2 = r_{\mathrm{g}}(\sin\psi_{\mathrm{n}} - \sin\theta_{\mathrm{g}}),$$
$$C_2 = \pm[r_{\mathrm{g}}(\cos\theta_{\mathrm{g}} - \cos\psi_{\mathrm{n}}) + D_0],$$

and r_2 and r_{g} are the radii of the elliptical pitch curve and the circular-arc rack cutter Σ_{g}, and θ_{g} is a design parameter of the rack cutter, Σ_{g}, used to determine the working region of the driven gear and limited by $\theta_{\mathrm{g}\min} \le \theta_{\mathrm{g}} \le \theta_{\mathrm{g}\max}$. According to Fig. 3, the bounds can be determined by the geometric relationship and are expressed as follows:

$$\theta_{\mathrm{g}\min} = \sin^{-1}\left(\frac{r_{\mathrm{g}}\sin\psi_{\mathrm{n}} - C_0}{r_{\mathrm{g}}}\right), \tag{22}$$

and

$$\theta_{\mathrm{g}\max} = \sin^{-1}\left(\frac{r_{\mathrm{g}}\sin\psi_{\mathrm{n}} - C_0 + C_1}{r_{\mathrm{g}}}\right). \tag{23}$$

5. Tooth undercutting

The relative velocity between the rack cutter surface and the generated gear can be represented in coordinate system $S_{\mathrm{c}}^{(\mathrm{p})}$ as,

$$\boldsymbol{V}_{\mathrm{c}}^{(\mathrm{c1})} = \boldsymbol{V}_{\mathrm{c}}^{(\mathrm{c})} - \boldsymbol{V}_{\mathrm{c}}^{(1)}, \tag{24}$$

where $\boldsymbol{V}_{\mathrm{c}}^{(\mathrm{c})} = \boldsymbol{V}_{\mathrm{c}}$ denotes the velocity of the rack cutter in coordinate system $S_{\mathrm{c}}^{(\mathrm{p})}$ while $\boldsymbol{V}_{\mathrm{c}}^{(1)}$ denotes the velocity of the generated gear. According to the generation mechanism presented in Fig. 4, the relative velocity of the tooth profiles of the circular-arc elliptical gear and the circular-arc rack cutter, expressed in Eq. (24), can be rewritten as follows:

$$\boldsymbol{V}_{\mathrm{c}}^{(\mathrm{c1})} = \omega_1[r_{\mathrm{p}}(\cos\theta_{\mathrm{p}} - \cos\psi_{\mathrm{n}}) + B_0 + S]\boldsymbol{i}_{\mathrm{c}} + \omega_1[r_{\mathrm{p}}(\sin\psi_{\mathrm{n}} - \sin\theta_{\mathrm{p}})]\boldsymbol{j}_{\mathrm{c}}. \tag{25}$$

According to gear theory, the surface tangent $\mathbf{T}$ exists at any regular point on the generated gear tooth surface, i.e., $\boldsymbol{T} \neq 0$. A singular point appears on the circular-arc elliptical gear profile when tooth undercutting occurs, and the tangent vector $\boldsymbol{T} = 0$ at this singular point. Restated, the relative velocity at a singular point on the generated tooth surface equals zero. From the relative velocity and the equation of meshing, gear tooth undercutting occurs when one of the following equations is satisfied [8]:

$$\begin{vmatrix} \dfrac{\mathrm{d}x_{\mathrm{c}}^{(\mathrm{p})}}{\mathrm{d}\theta_{\mathrm{p}}} & -V_{x\mathrm{c}}^{(\mathrm{c1})} \\ \dfrac{\partial f_1}{\partial\theta_{\mathrm{p}}} & -\dfrac{\partial f_1}{\partial\phi_1}\dfrac{\mathrm{d}\phi_1}{\mathrm{d}t} \end{vmatrix} = 0, \tag{26}$$

or

$$\begin{vmatrix} \dfrac{\mathrm{d}y_{\mathrm{c}}^{(\mathrm{p})}}{\mathrm{d}\theta_{\mathrm{p}}} & -V_{y\mathrm{c}}^{(\mathrm{c1})} \\ \dfrac{\partial f_1}{\partial\theta_{\mathrm{p}}} & -\dfrac{\partial f_1}{\partial\phi_1}\dfrac{\mathrm{d}\phi_1}{\mathrm{d}t} \end{vmatrix} = 0, \tag{27}$$

where f_1 represents the equation of meshing, $V_{x\mathrm{c}}^{(\mathrm{c1})}$ and $V_{y\mathrm{c}}^{(\mathrm{c1})}$ are the X and Y components of the relative velocity, respectively, and $x_{\mathrm{c}}^{(\mathrm{p})}$ and $y_{\mathrm{c}}^{(\mathrm{p})}$ are the X and Y components of the position vector of the rack cutter, respectively, expressed in coordinate system S_{c}. Moreover, the equation of meshing, f_1 (Eq. (17)), between the circular-arc rack cutter and the driving circular-arc elliptical gear, can be rewritten as

$$f(\theta_{\mathrm{p}}, \phi_1) = S - r_{\mathrm{p}}\frac{\sin(\theta_{\mathrm{p}} - \psi_{\mathrm{n}})}{\sin\theta_{\mathrm{p}}} + B_0. \tag{28}$$

Substituting Eqs. (25) and (28) into Eqs. (26) or (27), yields the condition for tooth undercutting as follows:

$$\frac{\partial S}{\partial\gamma_1} = \frac{r_{\mathrm{p}}(\sin\psi_{\mathrm{n}} - \sin\theta_{\mathrm{p}})\sin\psi_{\mathrm{n}}}{\sin^3\theta_{\mathrm{p}}}. \tag{29}$$

The rack cutter undercuts the gear tooth if the radius of curvature of the elliptical pitch curve, ρ, exceeds $\rho_{\min}$, since the minimum value of the working point is $\theta_{\mathrm{p}} = \theta_{\mathrm{p}\min}$, $\rho_{\min} = b_1^2/a_1$, and as Wu et al. [17] proposed, the minimum radius of curvature of the elliptical pitch curve $\rho_{\min}$ is obtained at both sides of the major-axis of the elliptical curve. Thus, Eq. (29) becomes

$$\rho = \frac{\partial S}{\partial\gamma_1} = \frac{r_{\mathrm{p}}(\sin\psi_{\mathrm{n}} - \sin\theta_{\mathrm{p}\min})\sin\psi_{\mathrm{n}}}{\sin^3\theta_{\mathrm{p}\min}} \ge \rho_{\min}. \tag{30}$$

Notably, the radius of curvature of the elliptical pitch curve must be limited to avoid tooth undercutting. Tooth undercutting usually occurs in the minimum curvature region, since the curvature of the elliptical pitch curve varies at each instantaneous pitch point.

6. Pointed teeth

The pointed teeth are an important issue in gear design and manufacture, especially for elliptical gears. The occurrence of pointed teeth reduces the gear addendum, instantaneous contact teeth, average contact ratio and gear strength. Pointed teeth appear if the top land radius, measured from the rotational center of the gear to the intersection point of the right- and left-sides of the gear surface profiles, is less than the radius of the gear addendum circle. Typically, the pointed teeth of an elliptical gear occur near its major-axis region. Based on the above concept, a profile index can be defined to check the occurrence of pointed teeth. Restated, the pointed teeth are generated when the distance, measured from the rotational center of the gear to the intersection point of the right- and left-side circular-arc tooth profiles at the major-axis, is less than the radius of the gear addendum circle near the gear's major-axis region. The circular-arc rack cutter will not produce a circular-arc elliptical gear with pointed teeth if that gear is designed such that the radius of its addendum circle at the major-axis is less than the radius of its pointed teeth.

7. Numerical examples

The mathematical models represented by Eqs. (16) and (20) are for the driving and driven circular-arc elliptical gears, respectively. Based on these models, this study develops a computer simulation to plot the graphs for the gears, and investigate the tooth undercutting and pointed teeth. Three examples clarify the influence of the design parameters on the surface profile of the circular-arc elliptical gear, and the means of obtaining a circular-arc elliptical gear without tooth undercutting and pointed teeth.

Example 1. The standard circular-arc rack cutters, as shown in Figs. 2 and 3, are designed to generate the driving and driven circular-arc elliptical gears, respectively. The gears are designed to have a pressure angle of $\psi_n = 20^\circ$ at the pitch point, a module of $m = 2.0$ mm/teeth and a major semi-axis of $a_1 = 30$ mm. The radii of the driving and driven circular-arc rack cutters are $r_p = 350$ and $r_g = 350$ mm, respectively. The number of teeth on the gear varies from 22 to 29.

The circumference of an elliptical gear must satisfy $S = \pi mT$, where T is the number of teeth. Otherwise, the generated elliptical gear will have an incomplete tooth. Therefore, the eccentricity of the circular-arc elliptical gear can be computed from Eq. (8) with $S = \pi mT$ and choosing an integral range from 0 to 2π. The radius of addendum circle at the major-axis r_a can be computed by substituting $\theta_{p\max} = \sin^{-1}((r_p \sin\psi_n - A_0 + 2m)/r_p)$ into Eq. (19) and considering the geometrical relationship shown in Fig. 2. The radius, r_{PT}, of the pointed tooth at the major-axis and the designed radius, ρ, can be calculated according to the proposed circular-arc elliptical gear mathematical models and the developed computer simulation program. Table 1 lists the relationships among the number of teeth T, eccentricity ε_1, minimum radius ρ_{min}, designed radius ρ, addendum radius r_a at the major-axis, and the calculated pointed tooth radius, r_{PT}. The minimum radius, ρ_{min}, of an elliptical gear should exceed the design radius, ρ, to prevent tooth undercutting, as explained in the previous section. Pointed teeth do not occur on the designed circular-arc elliptical gear, when the addendum circle radius r_a is less than the pointed tooth radius r_{PT} at the major-axis. Table 1 shows that the number of teeth, $T = 27$, corresponds to eccentricity $\varepsilon_1 = 0.608$, $\rho = 17.984$ mm, $\rho_{min} = 18.917$ mm, $r_a = 14.439$ mm, and $r_{PT} = 14.763$ mm. The designed driving circular-arc elliptical gear has neither tooth undercutting nor pointed teeth, since ρ_{min} exceeds ρ, and r_a is less than r_{PT}. Fig. 5 displays the generated tooth profile of the driving circular-arc elliptical gear while Fig. 6 illustrates the tooth profile of the driven circular-arc elliptical gear.

Recalling Table 1, the designed radius ρ exceeds the limiting value of the minimum radius of tooth undercutting ρ_{min} for a design with fewer than 27 teeth. Consequently, tooth undercutting occurs on tooth profiles of the designed circular-arc elliptical gear when the number of teeth is under 27. Moreover, pointed teeth occur when the number of teeth is under 26. Fig. 7 shows the computer graph of the circular-arc elliptical gear with $T = 24$ teeth, and both tooth undercutting and pointed teeth are observed.

Table 1
Calculated design parameters for circular-arc elliptical gears with pressure angle $\psi_n = 20^\circ$ and $r_p = 350$ mm under different number of teeth

	Number of teeth, T							
	29	28	27	26	25	24	23	22
Eccentricity, ε_1	0.361	0.503	0.608	0.692	0.762	0.821	0.872	0.916
Undercutting index								
ρ (mm)	17.984	17.984	17.984	17.984	17.984	17.984	17.984	17.984
ρ_{min} (mm)	26.101	22.405	18.917	15.643	12.589	9.764	7.179	4.853
Pointed teeth index								
r_a (mm)	21.693	17.488	14.439	12.032	10.068	8.442	7.071	5.837
r_{PT} (mm)	22.342	17.987	14.763	12.147	9.937	8.027	6.355	4.879

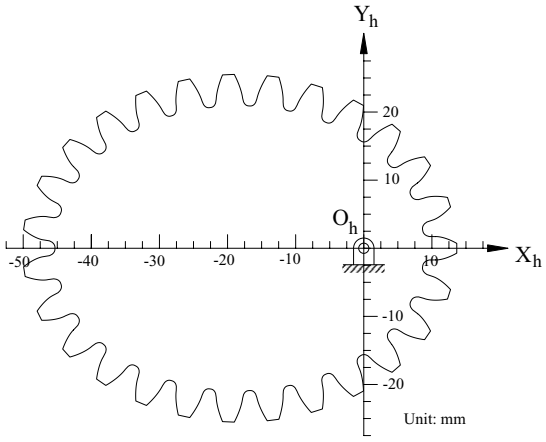

Fig. 5. Computer graph of the driving circular-arc elliptical gear.

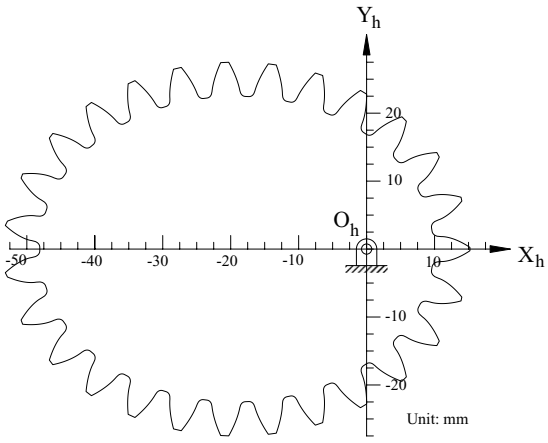

Fig. 6. Computer graph of the driven circular-arc elliptical gear.

Example 2. This example illustrates the effects of the gear pressure angle, ψ_n, on tooth undercutting and pointed teeth. The standard circular-arc rack cutters, shown in Figs. 2 and 3, are chosen to generate the mating gears with a module of $m = 2.0$ mm/teeth, number of teeth $T = 24$, length of major semi-axis $a_1 = 30$ mm, and radii of the rack cutter for generating the circular-arc driving and driven gears $r_p = 350$ and $r_g = 350$ mm, respectively. The pressure angle, ψ_n, is varied from 5° to 40°.

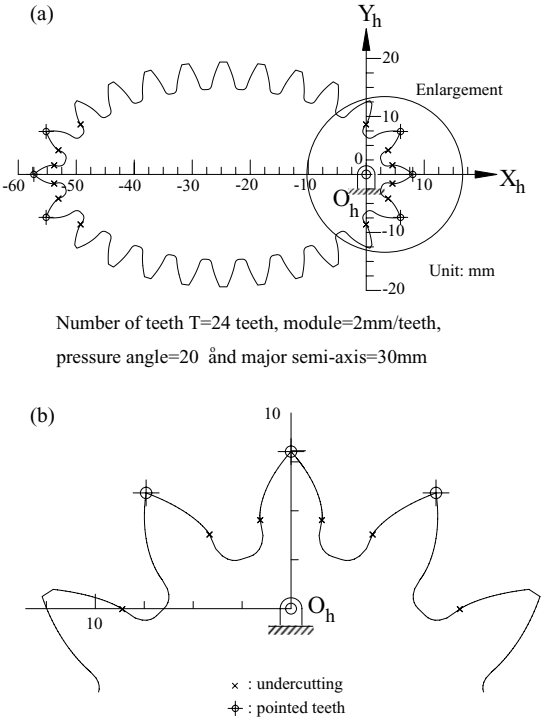

Fig. 7. (a) Circular-arc elliptical gear with tooth undercutting and pointed teeth. (b) Enlargement of the tooth undercutting and pointed teeth.

Table 2 shows the effects of pressure angle on tooth undercutting and pointed teeth, using the same calculation procedure as stated in Example 1. Increasing the pressure angle is found to decrease simultaneously the designed radius ρ, addendum radius r_a at the major-axis, and pointed teeth radius r_{PT}. Consider the case of choosing a pressure angle of $\psi_n = 30°$, some gear parameters can be calculated and obtained as follows: $r_T = 7.823$ mm, $r_{PT} = 7.519$ mm, $\rho_{min} = 9.764$ mm, and $\rho = 8.281$ mm. Tooth undercutting of the circular-arc elliptical gear does not occur because ρ_{min} is larger than ρ. However, pointed teeth appear on the generated tooth profile even if the pressure angle is increased to 40°.

Example 3. The same gear parameters in Example 2 are selected for the designed gears except that the circular-arc

Table 2
Calculated design parameters for the circular-arc elliptical gear of 24 teeth under different pressure angles

	Pressure angle, γ_n (°)							
	5	10	15	20	25	30	35	40
Eccentricity, ε_1	0.821	0.821	0.821	0.821	0.821	0.821	0.821	0.821
Undercutting index								
ρ (mm)	322.693	73.331	31.925	17.984	11.665	8.281	6.265	4.972
ρ_{min} (mm)	9.764	9.764	9.764	9.764	9.764	9.764	9.764	9.764
Pointed teeth index								
r_a (mm)	13.250	10.524	9.147	8.442	8.054	7.823	7.673	7.566
r_{PT} (mm)	8.598	8.459	8.261	8.027	7.775	7.519	7.269	7.032

Table 3
Calculated design parameters correspond to the circular-arc elliptical gear with number of teeth = 24, pressure angle $\psi_n = 20^\circ$, module $m = 2$ mm/teeth, and major semi-axis $a_1 = 30$ mm

	Radius of the circular-arc, r_p (mm)							
	50	150	250	350	550	750	950	2000
Eccentricity, ε_1	0.821	0.821	0.821	0.821	0.821	0.821	0.821	0.821
Undercutting index								
ρ (mm)	24.830	19.263	18.355	17.984	17.654	17.503	17.417	17.248
ρ_{min} (mm)	9.764	9.764	9.764	9.764	9.764	9.764	9.764	9.764
Pointed teeth index								
r_a (mm)	8.255	8.396	8.428	8.442	8.454	8.460	8.464	8.471
r_{PT} (mm)	7.980	8.017	8.024	8.027	8.030	8.031	8.032	8.034

radius r_p varies from 50 to 2000 mm. Table 3 lists the calculated results for gears with $T = 24$ teeth and a pressure angle, $\psi_n = 20^\circ$. Increasing the circular-arc radius, r_p, leads to an increase of the addendum circle, r_a, at major-axis but a decrease of the designed radius, ρ. Table 3 clearly shows that neither tooth undercutting nor pointed teeth of the generated tooth profile can be avoided merely by increasing the circular-arc radius, r_p, in the design process.

8. Conclusions

This study presented a mathematical model of the circular-arc elliptical gear, which rotates about one of its foci. A computer simulation program was also developed to plot graphs of the circular-arc elliptical gears. The effects of gear design parameters, such as the number of teeth, pressure angle at pitch point and circular-arc radius of the rack cutter, on tooth undercutting and pointed teeth of the generated circular-arc elliptical gears have also been examined. The simulated results are most helpful to gear designers in avoiding tooth undercutting and pointed teeth. The following conclusions are drawn.

(1) Eccentricity depends on the number of teeth. Choosing gears with more teeth can decrease the eccentricity of the elliptical pitch curves and increase the limiting value of the minimum radius of tooth undercutting, such that, tooth undercutting of the elliptical gears can be avoided. The phenomenon of pointed teeth can also be improved.
(2) Increasing the gear pressure angle notably decreases the design radius of tooth undercutting, and tooth undercutting can be prevented. However, increasing the pressure angle decreases the addendum circle of elliptical gears at the major-axis, and pointed teeth cannot be avoided even if the pressure angle is increased to 40°.
(3) Increasing the circular-arc radius of the rack cutters can decrease the designed radius and increase the addendum circle at the major-axis. Restated, tooth undercutting can be improved by increasing the circular-arc radius, but pointed teeth may still occur.

Acknowledgements

The authors would like to thank the National Science Council of the Republic of China for financially supporting a portion of this work under Contract No. NSC 89-2212-E-009-075. Our sincere thanks also go to Dr. Biing-Wen Bair, professor of National Lien Ho Institute of Technology, Miao Li, Taiwan, for his kind help in guidance of computer programs.

References

[1] F.H. Miller, C.H. Young, Proportions of elliptic gears for quick return mechanism, Prod. Eng. 16 (7) (1945) 462–464.
[2] T. Bernett, Elliptical gears for irregular motion, Mech. Eng. 89 (6) (1967) 33–39.
[3] H. Katori, K. Yokogawa, T. Hayashi, A simplified synthetic design method of pitch curves based on motion specifications for noncircular gears, Trans. Jpn. Soc. Mech. Eng. 60 (570) (1994) 668–674.
[4] S.H. Tong, C.H. Yang, Generation of identical noncircular pitch curves, ASME J. Mech. Des. 120 (1998) 337–341.
[5] F. Freudenstein, C.K. Chen, Variable-ratio chain drives with noncircular sprockets and minimum slack-theory and application, ASME J. Mech. Des. 113 (1991) 253–262.
[6] M. Kuczewski, Designing elliptical gears, Mach. Des. (1988) 166–168.
[7] T. Emura, A. Arakawa, A new steering mechanism using noncircular gears, JSME Int. J. Ser. II 35 (4) (1992) 604–610.
[8] F.L. Litvin, Gear Geometry and Applied Theory, Prentice-Hall, Englewood Cliffs, NJ, 1994.
[9] S.L. Chang, C.B. Tsay, L.I. Wu, Mathematical model and undercutting analysis of elliptical gears generated by rack cutters, Mech. Mach. Theory 31 (7) (1996) 879–890.
[10] G. Nieman, E. Heyer, Investigations of worm gears, VDI 95 (1953) 141–157.
[11] E. Wildhaber, US Patent 1 601 750 (5 October 1926), and VDI Berichte, No. 47 (1961).
[12] M.L. Novikov, USSR Patent 109 750 (1956).
[13] F.L. Litvin, C.B. Tsay, Helical gears with circular arc teeth: simulation of conditions of meshing and bearing contact, ASME J. Mech. Trans. Autom. Des. 107 (1985) 556–564.

[14] Y. Ariga, S. Nagata, Load capacity of a new W–N gear with basic rack of combined circular and involute profile, ASME J. Mech. Trans. Autom. Des. 107 (1985) 565–572.
[15] C.B. Tsay, Z.H. Fong, S. Tao, The mathematical model of Wildhaber–Novikov gears applicable to finite element stress analysis, J. Math. Comput. Model. 12 (8) (1989) 936–946.
[16] N.P. Chirons, Gear Design and Application, McGraw-Hill, New York, 1967.
[17] X. Wu, S. Wang, A. Yang, Non-circular gear CAD/CAM technology, in: Proceedings of the Eighth World Congress on the Theory of Machines and Mechanisms, Prague, Czechoslovakia, 1991, pp. 391–394.